biophysics COLAB

Curated Preprint
v2 • November 17, 2022
Peer Review Information

Reviewed Preprint
v1 • April 27, 2022

Chloride ions evoke taste sensations by binding to the extracellular ligand-binding domain of sweet/umami taste receptors

Nanako Atsumi, Keiko Yasumatsu, Yuriko Takashina, Chiaki Ito, Norihisa Yasui, Robert F. Margolskee, Atsuko Yamashita

Graduate School of Medicine, Dentistry and Pharmaceutical Sciences, Okayama University, Okayama, Japan • Oral Health Science Center, Tokyo Dental College, Tokyo • School of Pharmaceutical Sciences, Okayama University, Okayama, Japan • Monell Chemical Senses Center, Philadelphia, PA, USA

https://en.wikipedia.org/wiki/Open_access
Copyright information

Endorsement statement (17 November 2022)

The preprint by Atsumi *et al*. describes how chloride binding to sweet- and umami-sensing proteins (T1R taste receptors) can evoke taste sensation. The authors use an elegant combination of structural, biophysical and electrophysiological approaches to locate a chloride binding site in the ligand-binding domain of medaka fish T1r2a/3 receptors. They convincingly show that low mM concentrations of chloride induce conformational changes and, using single fiber recordings, establish that mouse chorda tympani nerves are activated by chloride in a T1R-dependent manner. This suggests that chloride binding to sweet receptors could mediate the commonly reported sweet taste sensation following ingestion of low concentrations of table salt. The findings will be of broad relevance to those studying taste sensation and ligand recognition in GPCRs.

(This endorsement by Biophysics Colab refers to version 2 of this preprint, which has been revised in response to peer review of version 1.)

Abstract

Salt taste sensation is multifaceted: NaCl at low or high concentrations is preferably or aversively perceived through distinct pathways. Cl^- is thought to participate in taste sensation through an unknown mechanism. Here we describe Cl^- ion binding and the response of taste receptor type 1 (T1r), a receptor family composing sweet/umami receptors. The T1r2a/T1r3 heterodimer from the medaka fish, currently the sole T1r amenable to structural analyses, exhibited a specific Cl^- binding in the vicinity of the amino-acid-binding site in the ligand-binding domain (LBD) of T1r3, which is likely conserved across species, including human T1r3. The Cl^- binding induced a conformational change in T1r2a/T1r3LBD at sub- to low-mM concentrations similar to canonical taste substances. Furthermore, oral Cl^- application to mice increased impulse frequencies of taste nerves connected to T1r-expressing taste cells and promoted their behavioral preferences attenuated by a T1r-specific blocker or T1r3

knock-out. These results suggest that the Cl^- evokes taste sensations by binding to T1r, thereby serving as another preferred salt taste pathway at a low concentration.

Introduction

The taste sensation is initiated by specific interactions between chemicals in food and taste receptors in taste buds in the oral cavity. In vertebrates, the chemicals are grouped into five ‘ basic modalities: sweet, umami, bitter, salty, and sour. This sensation occurs through taste [1] receptor recognition specific to a group of chemicals representing each taste modality (Taruno *et al*, 2021). Regarding the salty taste, the preferable taste, ~100 mM concentration of table salt, is evoked by specific interaction between the epithelial sodium channel (ENaC) and sodium ion (Chandrashekar *et al*, 2010) (Fig 1). Notably, salt sensation exhibits multifaced properties (Roper, 2015), thereby suggesting the existence of an adequate concentration range for salt intake to maintain the homeostasis of body fluid concentration. For example, high concentrations of salt over levels perceived as a preferred taste, such as ~500 mM, stimulate bitter and sour taste cells and are perceived as an aversive taste (Oka *et al*, 2013). Conversely, low salt concentrations under the “preferable” concentration, such as several mM to a hundred mM concentrations, are perceived as sweet by human panels (Bartoshuk *et al*, 1964; Bartoshuk *et al*, 1978; Cardello, 1979). However, its mechanism has never been extensively pursued.

The various impacts of the salt taste sensation indicate multiple salt detection pathways in taste buds (Roper, 2015). Moreover, another component of table salt, the chloride ion, participates in taste sensation because of the existence of the “anion effect”: the salty taste is most strongly perceived when the counter anion is a chloride ion (Ye *et al*, 1991). Several reports suggested a certain cellular/molecular machinery underlying anion-sensitive Na^+-detection or Cl^--detection, which is independent of ENaC (Lewandowski *et al*, 2016; Roebber *et al*, 2019). Indeed, a recent study indicated that transmembrane channel-like 4 (TMC4) expressed in taste buds involves high-concentration Cl^--sensation (Kasahara *et al*, 2021). Nevertheless, no candidate molecule capable of sensing low or preferable concentrations of Cl^- has been elucidated. Therefore, the complete understanding of salt taste sensation, including the mechanism of chloride ion detection, remains unclear.

Unlike salt taste sensation, those for nutrients as sugars, amino acids, and nucleotides are understood as sweet and umami sensations through specific receptor proteins (Li *et al*, 2002; Nelson *et al*, 2002; Nelson *et al*, 2001). Sweet and umami receptors are composed of taste receptor type 1 (T1r) proteins in the class C G protein-coupled receptor family. In humans, the T1r1/T1r3 heterodimer serves as the umami taste receptor and responds to amino acids as L-glutamate and aspartate, and nucleotides. In contrast, the T1r2/T1r3 heterodimer is the sweet taste receptor and responds to sugars. We previously elucidated the crystallographic structure of the medaka fish T1r2a/T1r3 extracellular ligand-binding domain (LBD) (Nuemket *et al*, 2017), which is currently the sole reported structure of T1rs. In the structure, the amino acid-binding was observed in the middle of the LBD of T1r2a and T1r3 subunits, which was consistent with the fact that T1r2a/T1r3 is an amino-acid receptor (Oike *et al*, 2007). Furthermore, chloride ion binding was found in the vicinity of the amino-acid binding site in T1r3 (Fig 2A). So far, the physiological significance of Cl^--binding for T1rs functions remains unexplored. Nevertheless, chloride ions regulate other receptors in class C G protein-coupled receptors (GPCRs), such as metabotropic glutamate receptors (mGluRs) and calcium-sensing receptors (CaSRs), and act as positive modulators for agonist binding (Eriksen & Thomsen, 1995; Kuang & Hampson, 2006; Liu *et al*, 2020; Tora *et al*, 2018; Tora *et al*, 2015). The potential effect of Cl^--binding on T1r receptor function is of significant interest under these conditions.

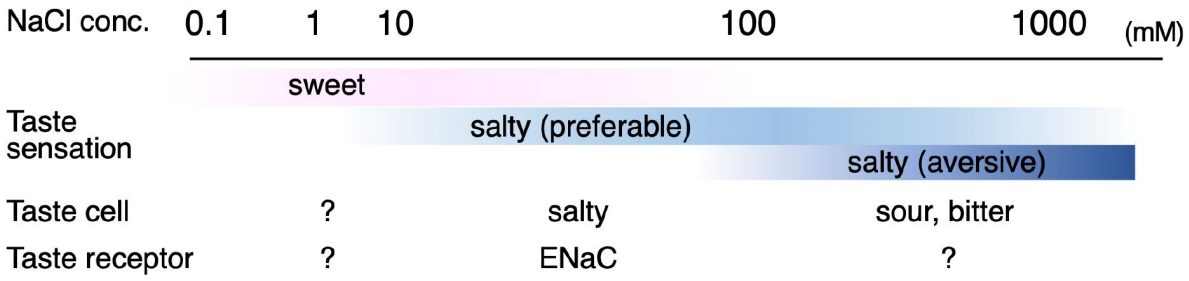

Figure 1.

Salt taste sensation.

Approximate concentration ranges of salt taste perceptions in humans (Bartoshuk *et al.*, 1978) and qualities of taste sensation with known cells and receptors responsible for their sensing are summarized.

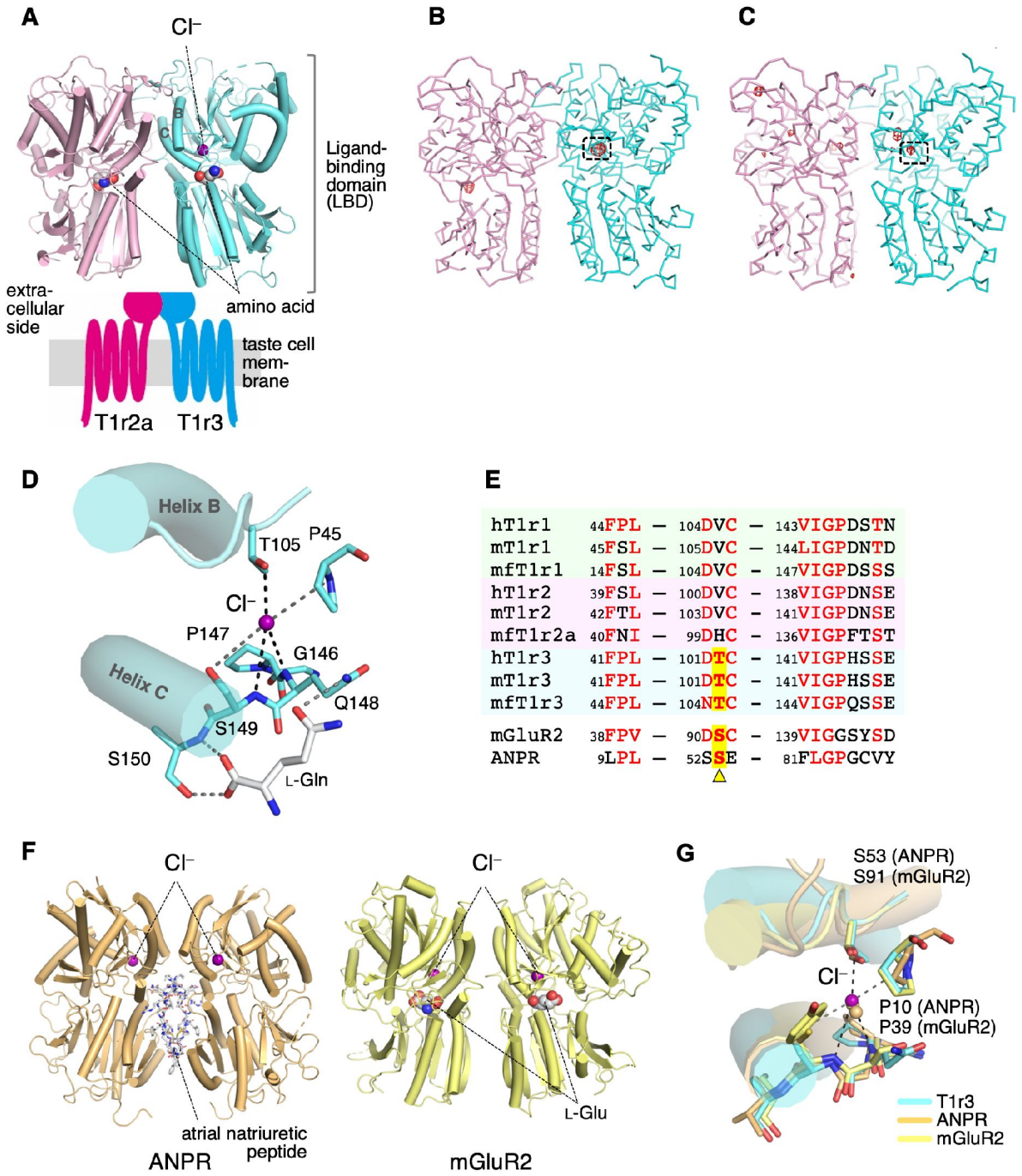

Figure 2.

Cl^--binding sites in the medaka fish taste receptor T1r2a/T1r3LBD.

Schematic drawing of the overall architecture of T1r2a/T1r3. The crystal structure (PDB ID: 5X2M) (Nuemket *et al*., 2017) is shown at the LBD region, and helices B and C in T1r3 are labeled. (B) Anomalous difference Fourier map (4.5 σ, red) of the Br^--substituted T1r2a/T1r3LBD crystal. (C) Anomalous difference Fourier map (4.5 σ, red) of the Cl -bound T1r2a/T1r3LBD crystal derived from the diffraction data collected at the wavelength of 2.7 Å. In panels B and C, the site originally identified the Cl^--binding was framed. (D) A close-up view of the Cl^--binding site in T1r3LBD in the Cl^--bound T1r2a/T1r3LBD (PDB ID: 5X2M). (E) Amino-acid sequence alignment of T1r proteins and the related receptors at the Cl^--binding site. The "h," "m," and "mf" prefixes to T1rs indicate human, mouse, and medaka fish, respectively. The position corresponding to Thr105 in T1r3 from medaka fish is highlighted. (F) The structures of ANPR (PDB ID: 1T34, left) (Ogawa *et al*, 2004) and mGluR2 (PDB ID: 5CNI, right) (Monn *et al*, 2015a) bound with Cl^-. (G) Superposition of the Cl^--binding site in T1r3, ANPR, and mGluR2.

Here, we investigated the Cl^- actions on T1rs using structural, biophysical, and physiological analyses. The Cl^- binding to the LBD was investigated using the medaka fish T1r2a/T1r3LBD, which is amenable to structural and biophysical analyses. Since the Cl^--binding site in T1r3 was conserved across various species, taste nerve recordings from mice were used to investigate the physiological significance of Cl^-. The results suggest that Cl^- induces the moderate response via T1rs, thereby implying that T1rs are involved in Cl^- sensation in taste buds.

Results

Cl^--binding site in T1r3

In the previously reported structure of T1r2a/T1r3LBD crystallized in the presence of NaCl, bound Cl^- was identified based on electron density and binding distances (Nuemket *et al*., 2017). To verify the Cl^--binding, Cl^- in the T1r2a/T1r3LBD crystal was substituted with Br^-, a halogen ion amenable for specific detection by anomalous scattering using a synchrotron light source (Table S1). The diffraction data from the crystal resulted in an anomalous difference Fourier peak at 14.1 σ at the site in the vicinity of the amino-acid binding site in T1r3, where Cl^- was originally bound (Fig 2B, S1A). For further confirmation, the anomalous data of the original crystal containing Cl^- was collected at 2.7 Å, where the anomalous peak for Cl and several other elements such as Ca or S can be detected (Table S1). The resultant anomalous difference Fourier map showed a peak at the bound Cl^- position, while all the other peaks were observed at the S atoms in the protein (Fig 2C, S1B). These results verify that the site is able to bind halogen ions, likely accommodating Cl^- under physiological conditions.

Cl^- was coordinated at the binding site by the side-chain hydroxyl group of Thr105 and the main-chain amide groups of Gln148 and Ser149 (Fig 2D). These main-chain coordinating residues are followed by Ser150, a critical residue for binding amino-acid ligands (Nuemket *et al*., 2017). Furthermore, the loop regions where Thr105 and the Gln148-Ser150 locate are followed by helices B and C, respectively. These helices are essential structural units at the heterodimer interface (Nuemket *et al*., 2017) (Fig 2A). They are known to reorient upon agonist binding, resulting in conformation rearrangement of the subunits in the dimer, likely inducing receptor activation in class C GPCRs (Koehl *et al*, 2019; Kunishima *et al*, 2000). In addition, the side-chain hydroxyl group of Ser149, which serves as a cap for the positive helix dipole of helix C, simultaneously functions as a distal ligand for Cl^- coordination. Therefore, the Cl^- binding at this site is important for organizing the structure of the amino-acid binding site and the heterodimer interface.

The Cl^--binding site observed in the crystal structure is most likely conserved among T1r3s in various organisms, such as humans (Fig 2E). Thr105, the residue that provides the side-chain-coordinating ligand for Cl^--binding, is strictly conserved as either serine or threonine among T1r3s. Additionally, the amino-acid sequence motifs surrounding the main-chain-coordinating ligands, $FP^{45}L$ and $VIGP\zeta^{148}\zeta^{149}$, where "$\zeta$" is a hydrophilic amino acid, are well conserved to present the main-chain amide groups to coordinate Cl^- with an appropriate geometry. Notably, the site structurally corresponds to the Cl^--binding site in the hormone-binding domain of the atrial natriuretic peptide receptor (ANPR) (Fig 2F, G), in which Cl^- positively regulates the peptide hormone binding (Misono, 2000). Although ANPR is not a member of class C GPCR, the hormone-binding domain in ANPR shares a similar structural fold with LBD of T1rs and other class C GPCRs, and bacterial periplasmic-binding proteins (Kunishima *et al*., 2000; van den Akker *et al*, 2000). Accordingly, the conservation of the structure and the sequence motif at the Cl^--binding site at ANPR is also observed on mGluRs (Ogawa *et al*, 2010). Indeed, Cl^- binding at the site corresponding to that in T1r3 was observed in several mGluR and CaSR structures (Monn *et al*, 2015b; Zhang *et al*, 2016) (Fig 2F, G) and was identified as a potential site responsible for regulating agonist binding (Liu *et al*., 2020; Tora *et al*., 2015). These results strongly imply the possibility that Cl^- has some actions on T1r receptor functions.

In contrast, conservation at the Thr105 position was not observed among T1r1 and T1r2 (Fig 2E). Evidently, no significant anomalous peak derived from Br^-- or Cl^--binding was observed in the crystal structure at the corresponding site in T1r2a (Fig 2B, C). His100 in T1r2a, which corresponds to Thr105 in T1r3, adopted a significantly different side-chain conformation from that of Thr105 in T1r3 (Fig S1C). Therefore, T1r1 and T1r2's ability to bind Cl^- is unlikely.

In addition to the Cl^--binding site discussed above, the Br^--substituted crystal exhibited an anomalous peak at 8.5 σ in T1r2a, at a position close to the Lys265 side-chain ε- amino group (Fig 2B, S1D). Nevertheless, Cl^--binding was not observed in the original Cl^--contained crystal. This is further confirmed by the absence of an anomalous peak at this position in the data collected at 2.7 Å (Fig 2C, S1E). Therefore, the site might have the ability to bind anions such as Br^- or larger; but be not specific to Cl^-. In human T1r1, the residue corresponding to Lys265 (Arg277) was suggested as a critical residue for activities of inosine monophosphate, an umami enhancer (Zhang *et al*, 2008).

Cl^--binding properties in T1r2a/T1r3LBD

To investigate the Cl^- actions on T1r functions, we first examined the properties of the Cl^--binding to medaka T1r2a/T1r3LBD using various biophysical techniques. For this purpose, the purified T1r2a/T1r3LBD was subjected to differential scanning fluorimetry (DSF), which we previously used for the amino acid-binding analysis (Yoshida *et al*, 2019). In order to prepare a Cl^--free condition, Cl^- in the sample was substituted with gluconate, as it is unlikely accommodated in the Cl^--site due to its much larger size. We confirmed that gluconate does not serve as a ligand for T1r2a/T1r3LBD (Fig S2A).

The addition of Cl^- to the Cl^--free T1r2a/T1r3LBD sample resulted in thermal stabilization of the protein (Fig 3A), which is indicative of Cl^- binding to the protein. The apparent K_d value for Cl^- estimated by the melting temperatures (T_m) at various Cl^- concentrations was ~110 μM (Fig 3B, Table 1). The Cl^--dependent thermal stabilization was confirmed by the fluorescence-detection size-exclusion chromatography-based thermostability (FSEC-TS) assay (Hattori *et al*, 2012) (Fig 3C, Table 1). However, the Cl^--dependent stabilization was not observed on T1r2a/T1r3 with the Cl^--site mutation, T105A in T1r3. In the case of this mutant, the T_m values for both in the presence and absence of Cl^- was similar to the values obtained for the wild-type protein in the absence of Cl^- (Fig 3C, S2B, Table 1). These results indicate that the Cl^- effect attributed to the identical site where the Cl^--binding was observed in the crystal structure of T1r3.

Next, we examined the consequence of the Cl^--binding to T1r2a/T1r3LBD via Förster resonance energy transfer (FRET) using the fluorescent protein-fused sample. Class C GPCRs commonly exhibit agonist-induced conformational changes in LBD, such as the dimer rearrangement, which is essential for receptor activation and signaling (Ellaithy *et al*, 2020; Koehl *et al*., 2019; Kunishima *et al*., 2000; Lin *etal*, 2021). Consistent with this, we previously reported that T1r2a/T1r3LBD shows conformational change concomitant with the binding of amino acids, which can be detected as increased FRET intensity (Nango *et al*, 2016). Notably, adding Cl^- to the fluorescent protein-fused T1r2a/T1r3LBD also increased FRET intensities, similar to amino acids (Fig 3D). The EC50 for Cl^--induced FRET signal change was determined as ~1 mM (Table 1). Note that both DSF and FRET estimations have some degree of error: the former produced slightly lower values than the latter, particularly in the case of weak affinities in the mM concentration range (Yoshida *et al*., 2019). As such, although the EC50 value determined by FRET was slightly higher than the apparent K_d value of Cl^- determined by DSF, the two are most likely relevant. Considering that the Cl^--binding site is located adjacent to the dimer interface, which exhibits reorientation upon agonist binding (Fig 2D), the results suggest that the Cl^-binding to T1r2a/T1r3LBD induces a conformational rearrangement of T1r2a/T1r3LBD similar to its agonist amino acid. Nevertheless, the extent of the FRET change induced by Cl^- was smaller than the changes induced by amino acids, such as ~1/2 of the latter (Fig 3E). Therefore, the results suggest

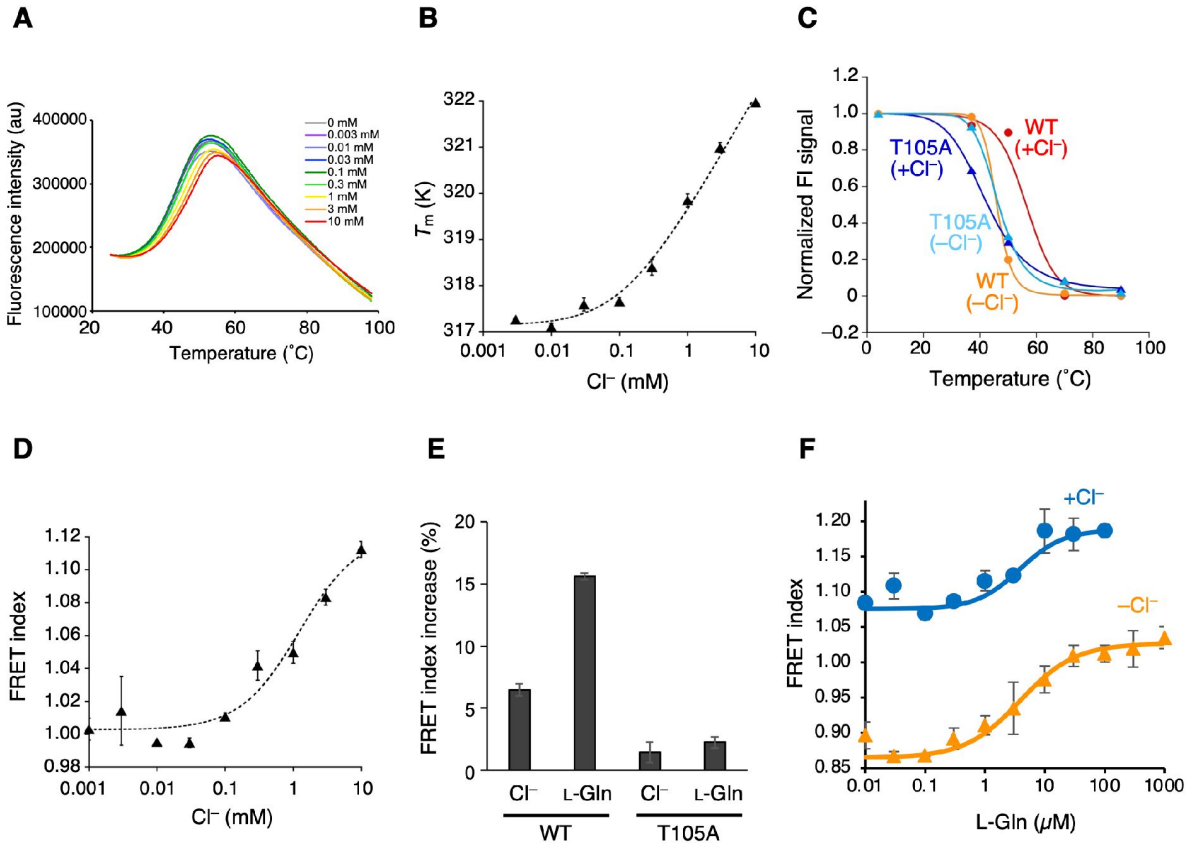

Figure 3.

The Cl^--binding properties of T1r2a/T1r3LBD.

(A) Representative thermal melt curves of T1r2a/T1r3LBD in the presence of 0.003 –10 mM concentrations of Cl^- measured using DSF. (B) Dose-dependent T_m changes of T1r2a/T1r3LBD by addition of Cl^-. (*n* = 4) (C) Thermal melting curves of WT and the T1r3-T105A mutant of T1r2a/T1r3LBD in the presence and absence of Cl^-, analyzed by FSEC-TS. (*n* = 1) (D) Dose-dependent FRET signal changes of the T1r2aLBD-Cerulean and T1r3LBD-Venus heterodimer by addition of Cl^-. (*n* = 3) (E) FRET index increases by adding 10-mM Cl^- or 1-mM L-glutamine to the WT or T1r3-T105A mutant T1r2aLBD-Cerulean/T1r3LBD-Venus heterodimer relative to that in the absence of any ligand in the absence of Cl^-. (*n* = 3) (F) Dose-dependent FRET signal changes of the T1r2aLBD-Cerulean and T1r3LBD-Venus heterodimer induced by the addition of L-glutamine in the presence and absence of Cl^-. (*n* = 3) The experiments were performed two (panels A, B, D, and E), three (C and WT), four (F and +Cl^- condition), or one (C and mutant; F and –Cl^- condition) time(s), and the results from one representative experiment are shown with numbers of technical replicates. Data points represent mean and s.e.m.

Cl^--binding, DSF (n = 4)		
$K_{d\text{-app}}$ (mM)	0.111 ± 0.046	
Protein thermal stability, DSF (n = 6)		
condition	+Cl^-	-Cl^-
Melting temperature (˚C)	55.2 ± 0.03	46.6 ± 0.06
Protein thermal stability, FSEC-TS		
wild type T1r2a/T1r3LBD (n = 3)		
condition	+Cl^-	-Cl^-
Melting temperature (˚C)	56.4 ± 5.1	46.0 ± 0.3
mutant T1r2a/T1r3-T105ALBD		
condition	+Cl^-	-Cl^-
Melting temperature (˚C)	42.7 ± 0.1	46.7 ± 0.7
Cl^-- binding, FRET (n = 3)		
FRET index minimum	1.00 ± 0.005	
FRET index change	0.119 ± 0.014	
EC_{50} (mM)*	1.23 ± 0.53	
L-glutamine binding, FRET (n = 3)		
condition	+Cl^-	-Cl^-
FRET index minimum	1.08 ± 0.01	0.86 ± 0.01
FRET index change	0.11	0.17
EC_{50} (μM)	3.78 ± 1.29	3.87 ± 1.76
Hill coefficient	1.20 ± 0.88	0.94 ± 0.29
L-glutamine binding, ITC		
condition	+Cl^-	-Cl^-
N (sites)	0.389 ± 0.028	0.303 ± 0.023
K_a (M^{-1})	(2.85 ± 0.65) × 10^5	(2.12 ± 0.46) × 10^5
[converted to K_d (μM)]	[3.51]	[4.72]
ΔH (kcal/mol)	-12.3 ± 1.2	–12.9 ± 1.3
ΔS (cal/mol/deg)	–16.3	-18.8

*Hill coefficient was fixed to 1 for fitting.

Table 1.

Properties of the Cl^--binding to T1r2a/T1r3LBD.

that the extent of the conformational change induced by Cl^- is smaller than the change induced by amino acids. The extent of Cl^--dependent FRET index change was reduced on T1r2a/T1r3 with the Cl^--site mutation, T105A in T1r3 (Fig 3E). Considering that the amino-acid-dependent change in the mutant was also significantly reduced (Fig 3E), the T105A mutation on T1r3 might result in losing the ability of the conformational change induced by Cl^--and amino-acid bindings, although the possibility of deactivation of the protein during preparation due to its low stability cannot be excluded.

In addition to the Cl^--binding effect, the Cl^- effect on amino-acid binding to T1r2a/T1r3LBD was investigated by FRET and isothermal calorimetry (ITC). The K_d values for L-glutamine binding determined by ITC, as well as the EC_{50} values and the other parameters for L-glutamine-induced conformational change determined by FRET, did not differ in the presence and absence of Cl^- (Fig 3F, S2C, 2D, and Table 1). These results indicated that the Cl^- binding had no significant effect on the binding of L-glutamine, a representative taste substance, at least for T1r2a/T1r3LBD from medaka fish.

Taste response to Cl^- through T1rs in mouse

Biophysical studies on T1r2a/T1r3LBD from medaka fish suggested that Cl^-binding to T1r3LBD induces a conformational change similar to that of an agonist without affecting agonist binding. As described above, the Cl^--binding site is likely conserved among T1r3 in various species, such as those in mammals. Therefore, we analyzed single fiber responses from mouse chorda tympani nerve to investigate the physiological effect of Cl^- on taste sensation. While conventional cell-based receptor assay systems are affected by changes in extracellular ionic components, the application of various solutions to the taste pore side of the taste buds projected to taste nerve systems, are transduced exclusively as “taste” signals, without inducing the other cellular responses derived from the ionic component changes in the surrounding environment.

We first identified nerve fibers that connect to T1r-expressing taste cells in wild-type (WT) mice, i.e., that receive taste information from cells likely possessing sweet (T1r2/T1r3) and umami (T1r1/T1r3) receptors (Yasumatsu *et al*, 2012). The identification was evidenced by responses to T1r agonists, such as sugars and amino acids, which were inhibited by gurmarin (Gur), a T1r-specific blocker (Daly *et al*, 2013; Margolskee *et al*, 2007; Ninomiya & Imoto, 1995; Ninomiya *et al*, 1999). Then, we examined the responses to Cl^- in these fibers. Remarkably, the fibers also exhibited responses induced by Cl^-, which was applied as a form of NMDG-Cl devoid of the known salty taste stimulant, sodium ion (Fig 4A). Cl^--induced impulse frequencies from the nerves increased in a concentration-dependent manner (Fig 4B). The responses to NMDG-Cl, NaCl, and KCl at the same concentrations did not differ significantly (repeated measures analysis of variance [ANOVA], $P > 0.05$), whereas responses to NMDG-gluconate were significantly smaller than those to NMDG-Cl (repeated measures ANOVA: $F(_{1, 43}) = 31.33$, $P < 0.001$) and did not induce explicit responses up to 10 mM. These results confirmed that the observed responses were attributed to Cl^-. All responses to Cl^-, regardless of the type of counter cations, were significantly decreased by lingual treatment with Gur (Fig 4B, repeated measures ANOVA: $F(_{1, 42}) = 56.65$, $P < 0.001$ for NMDG-Cl; $F(_{1, 50}) = 24.78$, $P < 0.001$ for NaCl; and $F(_{1, 45}) = 35.72$, $P < 0.001$ for KCl). Furthermore, responses to Cl^- in T1r3-KO mice were significantly lower than those in WT mice (repeated measures ANOVA: $F(_{1, 43}) = 25.36$, $P < 0.001$; Fig 4C). The results indicate that the observed Cl^--dependent responses were mediated by T1r. Notably, the Cl^--concentration range that induced nerve responses was lower (≤ ~10 mM) than that for Na^+-detection by ENaC when applied as the NaCl form (≥ ~30 mM) (Chandrashekar *et al*., 2010) but is consistent with those for Cl^--binding and Cl^--induced conformational change observed on T1r2a/T1r3LBD (Table 1). These results suggest that a low Cl^- concentration is sensorily detected via T1r in taste buds. Although the responses induced by known taste substances for T1rs, such as sugars and amino acids, range

from tens to hundreds of impulse frequencies per 10 s (Yasumatsu *et al*., 2012); the maximum response level induced by Cl^- was low, ~10 per 10 s (Fig 4B). According to our observations, Cl^- likely produces a "light" taste sensation compared with other known taste substances.

Next, to examine the physiological interaction between a canonical taste substance for mouse T1r and Cl^-, we recorded responses to 20-mM L-glutamine or 100-mM sucrose from T1r1/T1r3- and T1r2/T1r3-expressing cells, respectively, with or without NMDG-Cl from the same T1r-connecting single fibers (Fig 4A). The concentrations for the taste substances were set to induce responses greater than the baseline but less than maximum. As shown in Figure 4D, the response to L-glutamine or sucrose increased significantly by adding 10-mM NMDG-Cl (paired *t*-test, $t2 = 7.56$, $p = 0.017$ for L-glutamine and $t2 = 5.05$, $p = 0.037$ for sucrose). We confirmed that these responses had been suppressed by a lingual treatment of Gur in the presence ($t2 = 6.73$, $p = 0.021$ for L-glutamine and $t2 = 8.80$, $p = 0.013$ for sucrose) or absence ($t2 = 8.32$, $p = 0.014$ for L-glutamine and $t2 = 11.72$, $p = 0.007$ for sucrose) of NMDG-Cl to a similar extent. Moreover, the responses to the mixtures did not differ significantly from the summation of the responses to each solution ($t2 = 2.34$, $p = 0.145$ for L-glutamine and $t2 = 2.31$, $p = 0.147$ for sucrose). The results suggest that the simultaneous binding of Cl^- and a canonical taste substance, such as amino acids and sugars, to T1r do not cause synergistic responses.

Finally, we addressed whether T1r-mediated Cl^- responses observed in the taste nerves involve taste perception. Thus far, most reported behavioral assays for examining the gustatory detection of NaCl were performed with concentrations above ~30 mM, which can induce ENaC-mediated responses. Nevertheless, a few reports have shown that NaCl solution induced higher consumption relative to water even below 10-mM concentration (Dyr *et al*, 2014; Stewart *et al*, 1994), which is below the range inducing ENaC-mediated responses (Chandrashekar *et al*., 2010) but within what we observed in the Cl^--induced taste nerve responses via T1r. For verification, we performed a mouse two-bottle choice test using NMDG-Cl solution and analyzed the preference relative to water. The mouse preferred water containing 10-mM NMDG-Cl, which was abolished by the application of Gur (Fig 4E, F). These results suggest that Cl^- is preferably perceived through taste signal transduction mediated by T1r.

Discussion

In this study, Cl^- is found to specifically interact with the LBD in T1r3, a common component of sweet and umami taste receptors, and induces a conformational change in the receptor's LBD region. The Cl^- binding to T1r in taste cells is likely further transmitted to the sweet taste nervous system, resulting in a light yet preferable taste sensation. Since T1rs are conserved across vertebrates and the Cl^--binding site is likely conserved among T1r3 in various organisms, T1r-mediated Cl^- responses might be common in many animals, such as humans. Evidently, the concentration range for the Cl^--induced conformational change of medaka T1r2a/T1r3LBD and increase in murine sweet nerve impulses observed in this study (i.e., ≤ ~10 mM) agrees with the NaCl concentration perceived as "sweet" by humans (Bartoshuk *et al*., 1964; Bartoshuk *et al*., 1978; Cardello, 1979) (Fig 1). Additionally, the sweet sensation induced by NaCl was reportedly suppressed by topical application of *Gymnema sylvestre* (Bartoshuk *et al*., 1978), containing Gymnemic acids, which are specific inhibitors of human sweet taste receptor T1r2/T1r3 (Sanematsu *et al*, 2014). Overall, these results agree with the involvement of T1rs in the Cl^--taste detection. These findings agree with an earlier hypothesis by Bartoshuk and colleagues that dilute NaCl contains a sweet stimulus that interacts with the same receptor molecules as sucrose (Bartoshuk *et al*., 1978). The reported "sweet" sensation by low NaCl concentration faded out at the concentrations detected as "salty" (Bartoshuk *et al*., 1964; Bartoshuk *et al*., 1978; Cardello, 1979), thereby agreeing with the fact that we might be unaware that table salt is sweet at such

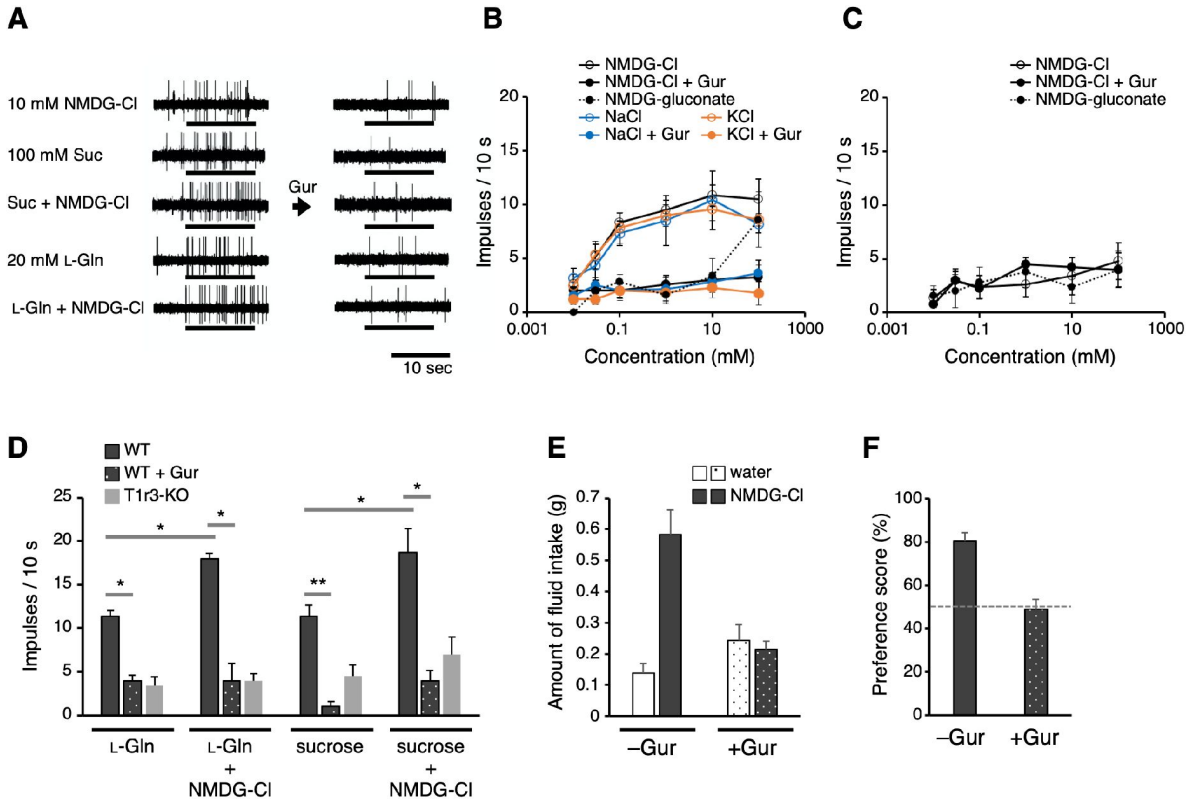

Figure 4.

Electrophysiological and behavioral analyses of the T1r-mediated Cl^- responses in mouse.

(A-D) Results of single fiber recordings from the mouse chorda tympani nerve. (A) Representative recordings of single fibers that connect to T1r-expressing taste cells. The stimuli were 10-mM NMDG-Cl, 100-mM sucrose, 100-mM sucrose + 10-mM NMDG-Cl, 20-mM L-glutamine, or 20-mM L-glutamine + 10-mM NMDG-Cl. Lines indicate the application of stimuli to the tongue. All the responses were suppressed by lingual treatment with a T1r blocker, Gur (right). (B) Impulse frequencies in response to the concentration series of NMDG-Cl, NaCl, or KCl before and after Gur treatment in WT mice. Responses to NMDG-gluconate are also shown. The mean number of net impulses per 10 s (mean response) ± s.e.m. in Gur-sensitive fibers (*n* = 5–6 from six mice). (C) Impulse frequencies in response to the concentration series of NMDG-Cl before and after Gur treatment were measured in T1r3-KO mice (*n* = 4-5 from three mice). Responses to NMDG-gluconate are also shown. (D) Impulse frequencies to 20-mM L-glutamine or 100-mM sucrose in the absence or presence of 10-mM NMDG-Cl before and after Gur treatment. Responses to 20-mM L-glutamine or 100-mM sucrose by T1r3-KO mouse are also shown. Values are mean ± s.e.m. (*n* = 3–5 from three mice each). *, **: paired *t*-test; $P < 0.05$ (*) and < 0.01 (**). (E) Amount of fluid intake for water and 10-mM NMDG-Cl in the two-bottle preference tests. Values are mean ± s.e.m. (*n* = nine mice) (F) NMDG-Cl intake shown in (E) normalized to water intake (preference score) in the two-bottle preference tests. A score > 50% indicates that the taste solution was preferred over water.

concentrations. The phenomenon could be explained by "mixture suppression" (Bartoshuk, 1975; Keast & Breslin, 2002; Stevens, 1996), such that a light sweet sensation is masked by an intense salty sensation in a higher concentration range of NaCl.

The Cl^- perception at low salt concentrations found in this study is achieved via the T1rs-mediating taste system, which transduces information as a preferred taste by nature. Since Cl^- is also a component of table salt, this system might serve as another pathway for preferred salt perception promoting intake along with the pathway for Na^+ perception as a preferred taste via taste cells that express the Na^+ receptor ENaC and a purinergic neurotransmission channel CALHM1/3 (Nomura *et al*, 2020). In contrast, the T1r-mediated Cl^--sensing observed in this study shows several different properties from those of cells or the molecules reportedly exhibiting anion-sensitive Na^+ detection or Cl^- detection in taste buds thus far. Specifically, the anion-sensitive Na^+-responding taste cells reported by Lewandowski *et al.* are type 3 cells, which include sour- but not sweet-responding cells (Lewandowski *et al*., 2016). The Cl^--detection pathway reported by Roebber *et al.* was observed in type 2 cells, which include both sweet- and bitter-responding cells, but was inhibited by a blocker of phospholipase C, which mediates sweet- and bitter-signaling downstream of T1r and bitter receptors (Roebber *et al*., 2019). The Cl^--responses mediated by TMC4 were observed in the glossopharyngeal nerve but not in the chorda tympani nerve wherein T1r-mediated responses were observed (Kasahara *et al*., 2021). Notably, responses by these reported pathways were tested by much higher concentrations of NaCl, typically in the several hundred mM range (Kasahara *et al*., 2021; Lewandowski *et al*., 2016; Roebber *et al*., 2019), than those used in this study. These results imply that there may be multiple distinct concentration-dependent pathways for Cl^- detection in taste buds. Given that high NaCl concentration is transduced as an aversive taste through bitter and sour taste cells (Oka *et al*., 2013), the relevance between the reported high Cl^--responsive pathways and high NaCl responses by bitter and sour cells is of interest, as pointed out by the previous studies, and will require further investigation.

Salt taste sensation and natriuresis are critical physiological processes that regulate sodium intake and excretion to maintain body fluid homeostasis. Intriguingly, both processes were found to use the counter anion Cl^- to regulate the molecular functions of the receptors, T1rs and ANPRs, which share a similar extracellular protein architecture with a conserved Cl^- -binding site. In the case of ANPR, mGluRs, and CaSR, positive allosteric modulations by Cl^- for agonist binding have been observed, with some variations in the extent of the enhancement (Eriksen & Thomsen, 1995; Kuang & Hampson, 2006; Liu *et al*., 2020; Tora *et al*., 2018; Tora *et al*., 2015). Whether the Cl^- actions on T1rs of other subtypes or from other organisms have some variance is yet to be examined.

Materials and methods

Crystallography

All protein samples used for structural and functional analyses were prepared using Drosophila S2 cells (Invitrogen) or high-expression clones for each protein sample established from S2 cells in previous studies (Nuemket *et al*., 2017; Yamashita *et al*, 2017). No authentication or test for mycoplasma contamination was performed.

The L-glutamine-bound T1r2a/T1r3LBD crystals, in complex with a crystallization chaperone Fab16A, were prepared in the presence of NaCl as described (Nuemket *et al*., 2017). For the preparation of the Br^--substituted crystals, the obtained crystals were soaked in a mother liquor consisting of 100 mM MES-Tris, pH 6.0, 50 mM NaBr, 17% PEG1500, 5% PEG400, 5 mM L-glutamine, 2 mM $CaCl_2$, cryoprotected by gradually increasing the concentration of glycerol to 10%, incubated for 2 hours, and flash-frozen.

The X-ray diffraction data were collected at the SPring-8 beamline BL41XU using a PILATUS6M detector (DECTRIS) at wavelength 0.9194 Å or at the Photon Factory beamline BL-1A using an EIGER X4M detector (DECTRIS) at wavelength 2.7 Å. The data were processed with XDS (Kabsch, 2010) (Table S1). The phases for anomalous difference Fourier map calculation were obtained by molecular replacement methods with the program PHASER (McCoy *et al*, 2007), using the structures of a single unit of the mfT1r2a-3LBD-Fab16A complex (PDB ID: 5X2M; ligands and water models were removed) (Nuemket *et al*., 2017) as the search model (the *R*/*R*free of the model for the Br^--data collected at 0.9194 Å: 0.248/0.350; the Cl^--data collected at 2.7 Å: 0.233/0.339).

Differential scanning fluorimetry (DSF)

Differential scanning fluorimetry was performed as previously described (Yoshida *et al*., 2019). The purified mfT1R2a/3LBD heterodimer protein was prepared (Nango *et al*., 2016) and dialyzed with buffer A (20 mM HEPES-NaOH, 300 mM sodium gluconate, pH 7.5) to remove Cl^-. 1 µg of the dialyzed protein sample was mixed with Protein Thermal Shift Dye (Applied Biosystems) and 0.003 – 10 mM NaCl in 20 µL of buffer A. The mixture solutions were then loaded to a MicroAmpR Fast Optical 48-Well Reaction Plate (Applied Biosystems). Fluorescent intensities were measured by the StepOne Real-Time PCR System (Applied Biosystems) while the temperature raised from 25 °C to 99 °C with a velocity of 0.022 °C/sec. For detection, the reporter and quencher were set as "ROX" and "none," respectively. The apparent melting transition temperature (*T*m) was determined using the maximum of the derivatives of the melt curve (dFluorescence/dT) by Protein Thermal Shift Software version 1.3 (Applied Biosystems). The apparent dissociation constant ($K_{d\text{-}app}$) for Cl^- derived from the T_m values at different NaCl concentrations was estimated using a thermodynamic model proposed by Schellman (Schellman, 1975) as described (Yoshida *et al*., 2019). The sample sizes for the analyses by DSF, as well as Förster resonance energy transfer and isothermal titration calorimetry described below, were set to obtain reliable values based on the experiences in the previous studies (Nango *et al*., 2016; Nuemket *et al*., 2017; Yoshida *et al*., 2019).

Förster resonance energy transfer (FRET)

FRET analysis was performed as described previously (Nango *et al*., 2016; Nuemket *et al*., 2017). The WT T1r2aLBD-Cerulean and T1r3LBD-Venus fusion heterodimer proteins were prepared as described (Nuemket *et al*., 2017). For the mutant protein preparation, a T1r3-T105A mutation was introduced into the vector pAc-mfT1r3aL-Ve (Nango *et al*., 2016) using polymerase chain reaction. The mutant expression vector was co-introduced with pAc-mfT1r2aL-Ce (Nango *et al*., 2016) to Drosophila S2 cells using Polyethyleneimine (PEI) "MAX" (Polysciences) as previously described (Bleckmann *et al*, 2019) with a ratio of 0.5-µg pAc-mfT1r2aL-Ce, 0.5-µg pAc-mfT1r3aL-Ve-T105A, and 10-µg PEI to ~1 × 10^6 cells. Protein expression and purification were conducted similarly as for the WT protein.

For the Cl^--titration, the purified protein samples were dialyzed against buffer A in the presence of 1-mM L-alanine. Afterward, the samples were diluted with buffer A to reduce the remaining L-alanine concentration below 1 µM (< ~1/100 of EC50 (Nango *et al*., 2016; Nuemket *et al*., 2017)), and then incubated in the presence of 0.001-10-µM NaCl or 1-mM L-glutamine in buffer A at 4°C overnight. For L-glutamine titration in the presence or absence of Cl^-, the protein solution was dialyzed with buffer B (20-mM HEPES-Tris, 300-mM NaCl, pH 7.5) or buffer C (20-mM HEPES-Tris, 300-mM sodium gluconate, pH 7.5) in the presence of 1-mM L-alanine to prepare the conditions with or without Cl^-, respectively. Then, the samples were diluted with buffer B or C to reduce the remaining L-alanine concentration below 1-µM and then incubated in the presence of 0.01-1000-µM L-glutamine at 4°C overnight. Fluorescence spectra were recorded at 298 K with a FluoroMax4 spectrofluorometer (Horiba). The sample was excited at 433 nm, and FRET was detected via the emission at 526 nm. The emission at 475 nm was also recorded for the FRET index

calculation. The FRET index (intensity at 526 nm/intensity at 475 nm) was plotted against the Cl^- or L-glutamine concentration, and the titration curves were fitted to the Hill equation using KaleidaGraph (Synergy Software) or ORIGIN (OriginLab).

Isothermal titration calorimetry

In order to prepare the conditions with or without Cl^-, the purified mfT1R2a/3LBD heterodimer protein was dialyzed with buffers B or C, respectively. The dialyzed protein solution (~50 μM) was then loaded into the sample cell in iTC200 (GE Healthcare) after the removal of insoluble materials by centrifugation (10,000×*g*, 15 min, 277 K). The titration was performed by injecting 2 μL of 400 μM L-glutamine at intervals of 120 s at 298 K. The thermograms and the binding isotherms were analyzed with Origin software, assuming one set of binding sites for fitting.

Fluorescence-detection size-exclusion chromatography-based thermostability assay (FSEC-TS)

A T1r3-T105A mutation was introduced in the vector pAc_mfT1r3L (Yamashita *et al*., 2017) by PCR. The mutant expression vector was co-introduced with pAc_mft1r2aL (Yamashita *et al*., 2017) to Drosophila S2 cells to establish a stable high-expression clone cell as previously described (Yamashita *et al*., 2017). The wild-type T1r2a/T1r3LBD and mutant T1r2a/T1r3-105A-LBD proteins were expressed and purified as previously described (Nango *et al*., 2016) with several modifications as listed below. After the protein binding to ANTI-FLAG M2 affinity gel, the resin was washed with either buffer D (20 mM HEPES-NaOH, 0.3 M NaCl, 2 mM CaCl2, 5 mM L-Gln, pH 7.5) or buffer E (20 mM HEPES-NaOH, 0.3 M Na gluconate, 2 mM Ca gluconate, 5 mM L-Gln, pH 7.5). Then, the protein was eluted with 100 μg/mL FLAG peptide in buffer D or E.

The protein solutions (50 μg/mL) in buffer D or E were incubated at 4 °C, 37 °C, 50 °C, 70 °C, or 90 °C at 2 hours. Subsequently, the samples were loaded on an SEC-5 column, 500 Å, 4.6 × 300 mm (Agilent) connected to a Prominence HPLC system (Shimadzu), using buffer D or E as a running buffer at a flow rate of 0.3 ml min^{-1}. The elution profiles were detected with an RF-20A fluorometer (Shimadzu), using excitation and emission wavelengths of 280 and 340 nm for the detection of intrinsic tryptophan fluorescence.

The residual ratio after incubation at each temperature was estimated using the fluorescence intensity at the elution peak, which corresponded to the T1rLBD dimer, *i.e*., the peak height at ~11.6 min. The values were normalized to the intensity of the sample incubated at 4 °C as 1. In order to estimate the apparent melting temperature ($T_{\text{m-app}}$) of the sample, the values of residual ratio at each temperature were fitted to the Gibbs-Helmholtz equation transformed as shown below (assuming that the sample protein is under equilibrium between a folding and unfolding state under each condition):

$$Residual\ ratio = 1 - \frac{1}{1 + exp\left[-\frac{\Delta H\left(1 + \frac{T}{T_{m-app}}\right) - \Delta C_P\left\{\left(T_{m-app} - \mathrm{T}\right) + Tln\left(\frac{T}{T_{m-app}}\right)\right\}}{RT}\right]}$$

where ΔH and ΔCp are the enthalpy and heat capacity change of unfolding, respectively; T is the temperature of the sample incubation; R is the gas constant. The fittings were performed with KaleidaGraph (Synergy Software), with ΔH, ΔC_{p}, and $T_{\text{m-app}}$ are set as valuables.

Single fiber recording from mouse chorda tympani (CT) nerve

All animal experiments were conducted following the National Institutes of Health Guide for the Care and Use of Laboratory Animals and approved by the committee for Laboratory Animal Care and Use and the local ethics committee at Tokyo Dental College and Okayama University Japan. The subjects were six adult male C57BL/6JCrj mice (Charles River Japan, Tokyo, Japan) and four

T1r3GFP-KO mice, which were obtained by mating T1r3-GFP (Damak *et al*, 2008) and T1r3-KO (Damak *et al*, 2003) mice. Mice were maintained on a 12/12-h light/dark cycle and fed standard rodent chow and 8-20 weeks of age ranging in weight from 20 g to 30 g.

The mice were anesthetized with an injection of sodium pentobarbital (40-50 mg/kg ip) and maintained at a surgical level of anaesthesia, with additional injections (8-10 mg/kg ip every hour). Under anaesthesia, each mouse was fixed in the supine position with a head holder, and the trachea cannulated. The right CT nerve was dissected, free from surrounding tissues, after the removal of the pterygoid muscle and cut at the point of its entry to the tympanic bulla. A single or a few nerve fibers were teased apart with a pair of needles and lifted onto an Ag-AgCl electrode, and an indifferent electrode was placed in nearby tissue. Their neural activities were amplified (K-1; Iyodenshikagaku, Nagoya, Japan) and recorded on a computer using a PowerLab system (PowerLab/sp4; AD Instruments, Bella Vista, NSW, Australia). For taste stimulation of fungiform papillae, the anterior half of the tongue was enclosed in a flow chamber. Taste solutions or rinses (distilled water) (~24 °C) were delivered to the tongue by gravity flow at the same flow rate (~0.1 mL s^{-1}). For data analysis, we used the net average frequency for 10 sec after the stimulus onset, which was obtained by subtracting the spontaneous frequency for the 10 sec duration before stimulation from after stimulation. In the initial survey to identify a nerve fiber connecting to T1r-expressing cells, test stimuli such as 100 mM NaCl, 10 mM HCl, 500 mM sucrose, 100 mM monopotassium glutamate, 20 mM quinine HCl were separately applied. If the fiber responded to sucrose, we applied 10 μM–100 mM NMDG-Cl, NaCl, KCl, or either of 20 mM L-glutamine or 100 mM sucrose with or without 10 mM NMDG-Cl to the tongue. The criteria for the occurrence of response were the following: the number of spikes was larger than the mean + two standard deviations of the spontaneous discharge for three 10-s periods before stimulation, and at least three spikes were evoked by taste stimulation (Yasumatsu *et al*., 2012). In the case of T1r3GFP-KO mice, as the mice showed a significant response to 0.5-M sucrose, we could identify sweet-responsive fibers (impulse frequency of 13.4 ± 1.31) (Yasumatsu *et al*., 2012). The reagents used were purchased from Wako Pure Chemical Industries (Osaka, Japan; others). To block responses via T1r (Daly *et al*., 2013; Margolskee *et al*., 2007; Ninomiya & Imoto, 1995; Ninomiya *et al*., 1999), each tongue was treated with 30-μg ml^{-1} (~7 μM) gurmarin (Gur) dissolved in 5-mM phosphate buffer (pH 6.8) for 10 min, similarly as described by Ninomiya & Imoto (Ninomiya & Imoto, 1995). To assure the detection of responses from T1r-expressing cells, recordings from Gurinsensitive sweet-responsive fibers were defined as those retaining impulse frequencies to 0.5-M sucrose more than 60% after the Gur treatment (Ninomiya *et al*., 1999) were excluded from the data. The number of Gur-sensitive and Gur-insensitive fibers were six and three, respectively, among 0.5-M sucrose responding fibers. The sucrose application was repeated 3–6 times during the recordings. Additionally, the recovery of the suppressed responses was confirmed using 15-mM β-cyclodextrin, which could remove the effect of Gur from the tongue (Ninomiya *et al*., 1999). All Gur-sensitive fibers recovered up to 60%–150% of responses before Gur. At the end of the experiment, animals were killed by administering an overdose of the anaesthetic. Repeated measures ANOVA and Student's paired *t*-test were used to statistically evaluate the effects of chemicals or gene deletion. The sample size was calculated according to power analysis, thereby resulting in three per group due to the effect size (d) of 6–9.3 to detect the effects of blocking or deleting T1r3.

Two-bottle preference tests

All training and testing sessions occurred during the light phase of the light/dark cycle. On the first day of training, the WT mice (adult male C57BL/6JCrj) were water deprived for 23 h and then placed in a test box with two bottles: one filled with water and the other empty. The amount of fluid intake was measured after a 5-min presentation. After 4 days of training, mice were used for test sessions if they drank water evenly on either side (nine mice). In the test sessions, they were

provided with two bottles, one containing 10-mM NMDG-Cl and the other containing water, with or without Gur, for 5 min. The amount of liquid consumed was measured by weighing the bottles, and a preference score of NMDG-Cl was calculated using the following equation:

$$Preference\ score(\%) = \frac{V_{Cl}}{V_{Cl} + V_w} \times 100$$

where V_{cl} and V_w are the amount of NMDG-Cl intake and water intake, respectively.

Supporting information

Figures S1, S2, and Table S1

Acknowledgements

We thank Drs. Kazuya Hasegawa, Nobuhiro Mizuno, Naohiro Matsugaki for help with X-ray data collection; Junya Nitta and Hikaru Ishida for help with protein preparation; Ryusuke Yoshida for help with the single fiber recording; Yuko Kusakabe for attempt at cell-based receptor assay in the early stage of the study; Haruo Ogawa for sharing knowledge about ANPR; Yuzo Ninomiya for valuable discussions. We also thank the reviewers of BioPhysics Colab for their helpful comments and Enago (www.enago.jp) for the English language review. The synchrotron radiation experiments at the BL41XU, SPring-8 were performed with approvals of the Japan Synchrotron Radiation Research Institute (JASRI) (Proposal No. 2016B2534). The synchrotron radiation experiment at the BL-1A, Photon Factory was supported by the Platform for Drug Discovery, Informatics, and Structural Life Science (Proposal No. 1264). This work was financially supported by JSPS KAKENHI Grant Numbers JP17H03644, JP18H04621, JP20H03195, JP20H04778, JP21H05524 (to A.Y) and JP20H03855 (to K.Y.), Mishima Kaiun Memorial Foundation, and the Salt Science Research Foundation (Proposal No. 2039) (to A.Y.).

Competing interests

The authors declare that they have no conflict of interest.

References

Bartoshuk LM (1975) **Taste mixtures: is mixture suppression related to compression?** *Physiol Behav* **14**:643–649 Google Scholar

Bartoshuk LM, McBurney DH, Pfaffmann C (1964) **Taste of Sodium Chloride Solutions after Adaptation to Sodium Chloride: Implications for the "Water Taste** *Science* **143**:967–968 Google Scholar

Bartoshuk LM, Murphy C, Cleveland CT (1978) **Sweet taste of dilute NaCl: psychophysical evidence for a sweet stimulus** *Physiol Behav* **21**:609–613 Google Scholar

Bleckmann M, Schurig M, Endres M, Samuels A, Gebauer D, Konisch N, van den Heuvel J (2019) **Identifying parameters to improve the reproducibility of transient gene expression in High Five cells** *PLoS One* **14**:e0217878 Google Scholar

Cardello AV (1979) **Taste quality changes as a function of salt concentration in single human taste papillae** *Chem Senses* **4**:1–13 Google Scholar

Chandrashekar J, Kuhn C, Oka Y, Yarmolinsky DA, Hummler E, Ryba NJ, Zuker CS (2010) **The cells and peripheral representation of sodium taste in mice** *Nature* **464**:297–301 Google Scholar

Daly K, Al-Rammahi M, Moran A, Marcello M, Ninomiya Y, Shirazi-Beechey SP (2013) **Sensing of amino acids by the gut-expressed taste receptor T1R1-T1R3 stimulates CCK secretion** *Am J Physiol Gastrointest Liver Physiol* **304**:G271–282 Google Scholar

Damak S, Mosinger B, Margolskee RF (2008) **Transsynaptic transport of wheat germ agglutinin expressed in a subset of type II taste cells of transgenic mice** *BMCNeurosci* **9**:96 Google Scholar

Damak S, Rong M, Yasumatsu K, Kokrashvili Z, Varadarajan V, Zou S, Jiang P, Ninomiya Y, Margolskee RF (2003) **Detection of sweet and umami taste in the absence of taste receptor T1r3** *Science* **301**:850–853 Google Scholar

Dyr W, Wyszogrodzka E, Mierzejewski P, Bienkowski P (2014) **Drinking of flavored solutions by high preferring (WHP) and low preferring (WLP) alcohol-drinking rats** *Pharmacol Rep* **66**:28–33 Google Scholar

Ellaithy A, Gonzalez-Maeso J, Logothetis DA, Levitz J (2020) **Structural and Biophysical Mechanisms of Class C G Protein-Coupled Receptor Function** *Trends Biochem Sci* **45**:1049–1064 Google Scholar

Eriksen L, Thomsen C (1995) **[3H]-L-2-amino-4-phosphonobutyrate labels a metabotropic glutamate receptor, mGluR4a** *Br J Pharmacol* **116**:3279–3287 Google Scholar

Hattori M, Hibbs RE, Gouaux E (2012) **A fluorescence-detection size-exclusion chromatography-based thermostability assay for membrane protein precrystallization screening** *Structure* **20**:1293–1299 Google Scholar

Kabsch W (2010) **Xds** *Acta Crystallogr D Biol Crystallogr* **66**:125–132 Google Scholar

Kasahara Y, Narukawa M, Ishimaru Y, Kanda S, Umatani C, Takayama Y, Tominaga M, Oka Y, Kondo K, Kondo T, et al (2021) **TMC4 is a novel chloride channel involved in high-concentration salt taste sensation** *J Physiol Sci* **71**:23 Google Scholar

Keast RS, Breslin PA (2002) **An overview of binary taste–taste interactions** *Food Quality and Preference* **14**:111–124 Google Scholar

Koehl A, Hu H, Feng D, Sun B, Zhang Y, Robertson MJ, Chu M, Kobilka TS, Laeremans T, Steyaert J, et al (2019) **Structural insights into the activation of metabotropic glutamate receptors** *Nature* **566**:79–84 Google Scholar

Kuang D, Hampson DR (2006) **Ion dependence of ligand binding to metabotropic glutamate receptors** *Biochem Biophys Res Commun* **345**:1–6 Google Scholar

Kunishima N, Shimada Y, Tsuji Y, Sato T, Yamamoto M, Kumasaka T, Nakanishi S, Jingami H, Morikawa K (2000) **Structural basis of glutamate recognition by a dimeric metabotropic glutamate receptor** *Nature* **407**:971–977 Google Scholar

Lewandowski BC, Sukumaran SK, Margolskee RF, Bachmanov AA (2016) **Amiloride-Insensitive Salt Taste Is Mediated by Two Populations of Type III Taste Cells with Distinct Transduction Mechanisms** *J Neurosci* **36**:1942–1953 Google Scholar

Li X, Staszewski L, Xu H, Durick K, Zoller M, Adler E (2002) **Human receptors for sweet and umami taste** *Proc Natl Acad Sci U S A* **99**:4692–4696 Google Scholar

Lin S, Han S, Cai X, Tan Q, Zhou K, Wang D, Wang X, Du J, Yi C, Chu X, et al (2021) **Structures of Gi-bound metabotropic glutamate receptors mGlu2 and mGlu4** *Nature* **594**:583–588 Google Scholar

Liu H, Yi P, Zhao W, Wu Y, Acher F, Pin JP, Liu J, Rondard P (2020) **Illuminating the allosteric modulation of the calcium-sensing receptor** *Proc Natl Acad Sci U S A* **117**:21711–21722 Google Scholar

Margolskee RF, Dyer J, Kokrashvili Z, Salmon KS, Ilegems E, Daly K, Maillet EL, Ninomiya Y, Mosinger B, Shirazi-Beechey SP (2007) **T1R3 and gustducin in gut sense sugars to regulate expression of Na+-glucose cotransporter 1** *Proc Natl Acad Sci U S A* **104**:15075–15080 Google Scholar

McCoy AJ, Grosse-Kunstleve RW, Adams PD, Winn MD, Storoni LC, Read RJ (2007) **Phaser crystallographic software** *J Appl Crystallogr* **40**:658–674 Google Scholar

Misono KS (2000) **Atrial natriuretic factor binding to its receptor is dependent on chloride concentration: A possible feedback-control mechanism in renal salt regulation** *Circ Res* **86**:1135–1139 Google Scholar

Monn JA, Prieto L, Taboada L, Hao J, Reinhard MR, Henry SS, Beadle CD, Walton L, Man T, Rudyk H, et al (2015a) **Synthesis and Pharmacological Characterization of C4-(Thiotriazolyl)-substituted-2-aminobicyclo[3.1.0]hexane-2,6-dicarboxylates. Identification of (1R,2S,4R,5R,6R)-2-Amino-4-(1H-1,2,4-triazol-3-ylsulfanyl)bicyclo[3.1.0]hexane-2, 6-dicarboxylic Acid (LY2812223), a Highly Potent, Functionally Selective mGlu2 Receptor Agonist** *J Med Chem* **58**:7526–7548 Google Scholar

Monn JA, Prieto L, Taboada L, Pedregal C, Hao J, Reinhard MR, Henry SS, Goldsmith PJ, Beadle CD, Walton L, et al (2015b) **Synthesis and pharmacological characterization of C4-disubstituted analogs of 1S,2S,5R,6S-2-aminobicyclo[3.1.0]hexane-2,6-dicarboxylate: identification of a potent, selective metabotropic glutamate receptor agonist and determination of agonist-bound human mGlu2 and mGlu3 amino terminal domain structures** *J Med Chem* **58**:1776–1794 Google Scholar

Nango E, Akiyama S, Maki-Yonekura S, Ashikawa Y, Kusakabe Y, Krayukhina E, Maruno T, Uchiyama S, Nuemket N, Yonekura K, et al (2016) **Taste substance binding elicits conformational change of taste receptor T1r heterodimer extracellular domains** *Sci Rep* **6**:25745 Google Scholar

Nelson G, Chandrashekar J, Hoon MA, Feng L, Zhao G, Ryba NJ, Zuker CS (2002) **An aminoacid taste receptor** *Nature* **416**:199–202 Google Scholar

Nelson G, Hoon MA, Chandrashekar J, Zhang Y, Ryba NJ, Zuker CS (2001) **Mammalian sweet taste receptors** *Cell* **106**:381–390 Google Scholar

Ninomiya Y, Imoto T (1995) **Gurmarin inhibition of sweet taste responses in mice** *Am J Physiol* **268**:R1019–1025 Google Scholar

Ninomiya Y, Imoto T, Sugimura T (1999) **Sweet taste responses of mouse chorda tympani neurons: existence of gurmarin-sensitive and-insensitive receptor components** *J Neurophysiol* **81**:3087–3091 Google Scholar

Nomura K, Nakanishi M, Ishidate F, Iwata K, Taruno A (2020) **All-Electrical Ca(2+)-Independent Signal Transduction Mediates Attractive Sodium Taste in Taste Buds** *Neuron* **106**:816–829 Google Scholar

Nuemket N, Yasui N, Kusakabe Y, Nomura Y, Atsumi N, Akiyama S, Nango E, Kato Y, Kaneko MK, Takagi J, et al (2017) **Structural basis for perception of diverse chemical substances by T1r taste receptors** *Nat Commun* **8**:15530 Google Scholar

Ogawa H, Qiu Y, Ogata CM, Misono KS (2004) **Crystal structure of hormone-bound atrial natriuretic peptide receptor extracellular domain: rotation mechanism for transmembrane signal transduction** *J Biol Chem* **279**:28625–28631 Google Scholar

Ogawa H, Qiu Y, Philo JS, Arakawa T, Ogata CM, Misono KS (2010) **Reversibly bound chloride in the atrial natriuretic peptide receptor hormone-binding domain: possible allosteric regulation and a conserved structural motif for the chloride-binding site** *Protein Sci* **19**:544–557 Google Scholar

Oike H, Nagai T, Furuyama A, Okada S, Aihara Y, Ishimaru Y, Marui T, Matsumoto I, Misaka T, Abe K (2007) **Characterization of ligands for fish taste receptors** *J Neurosci* **27**:5584–5592 Google Scholar

Oka Y, Butnaru M, von Buchholtz L, Ryba NJ, Zuker CS (2013) **High salt recruits aversive taste pathways** *Nature* **494**:472–475 Google Scholar

Roebber JK, Roper SD, Chaudhari N (2019) **The Role of the Anion in Salt (NaCl) Detection by Mouse Taste Buds** *J Neurosci* **39**:6224–6232 Google Scholar

Roper SD (2015) **The taste of table salt** *Pflugers Arch* **467**:457–463 Google Scholar

Sanematsu K, Kusakabe Y, Shigemura N, Hirokawa T, Nakamura S, Imoto T, Ninomiya Y (2014) **Molecular mechanisms for sweet-suppressing effect of gymnemic acids** *J Biol Chem* **289**:25711–25720 Google Scholar

Schellman JA (1975) **Macromolecular Binding** *Biopolymers* **14**:999–1018 Google Scholar

Stevens JC (1996) **Detection of tastes in mixture with other tastes: issues of masking and aging** *Chem Senses* **21**:211–221 Google Scholar

Stewart RB, Russell RN, Lumeng L, Li TK, Murphy JM (1994) **Consumption of sweet, salty, sour, and bitter solutions by selectively bred alcohol-preferring and alcohol-nonpreferring lines of rats** *Alcohol Clin Exp Res* **18**:375–381 Google Scholar

Taruno A, Nomura K, Kusakizako T, Ma Z, Nureki O, Foskett JK (2021) **Taste transduction and channel synapses in taste buds** *Pflugers Arch* **473**:3–13 Google Scholar

Tora AS, Rovira X, Cao AM, Cabaye A, Olofsson L, Malhaire F, Scholler P, Baik H, Van Eeckhaut A, Smolders I, et al (2018) **Chloride ions stabilize the glutamate-induced active state of the metabotropic glutamate receptor 3** *Neuropharmacology* **140**:275–286 Google Scholar

Tora AS, Rovira X, Dione I, Bertrand HO, Brabet I, De Koninck Y, Doyon N, Pin JP, Acher F, Goudet C (2015) **Allosteric modulation of metabotropic glutamate receptors by chloride ions** *FASEB J* **29**:4174–4188 Google Scholar

van den, Akker F, Zhang X, Miyagi M, Huo X, Misono KS, Yee VC (2000) **Structure of the dimerized hormone-binding domain of a guanylyl-cyclase-coupled receptor** *Nature* **406**:101–104 Google Scholar

Yamashita A, Nango E, Ashikawa Y (2017) **A large-scale expression strategy for multimeric extracellular protein complexes using Drosophila S2 cells and its application to the recombinant expression of heterodimeric ligand-binding domains of taste receptor** *Protein Sci* **26**:2291–2301 Google Scholar

Yasumatsu K, Ogiwara Y, Takai S, Yoshida R, Iwatsuki K, Torii K, Margolskee RF, Ninomiya Y (2012) **Umami taste in mice uses multiple receptors and transduction pathways** *J Physiol* **590**:1155–1170 Google Scholar

Ye Q, Heck GL, DeSimone JA (1991) **The anion paradox in sodium taste reception: resolution by voltage-clamp studies** *Science* **254**:724–726 Google Scholar

Yoshida T, Yasui N, Kusakabe Y, Ito C, Akamatsu M, Yamashita A (2019) **Differential scanning fluorimetric analysis of the amino-acid binding to taste receptor using a model receptor protein, the ligand-binding domain of fish T1r2a/T1r3** *PLoS One* **14**:e0218909 Google Scholar

Zhang C, Zhang T, Zou J, Miller CL, Gorkhali R, Yang JY, Schilmiller A, Wang S, Huang K, Brown EM, et al (2016) **Structural basis for regulation of human calcium-sensing receptor by magnesium ions and an unexpected tryptophan derivative co-agonist** *Sci Adv* **2**:e1600241 Google Scholar

Zhang F, Klebansky B, Fine RM, Xu H, Pronin A, Liu H, Tachdjian C, Li X (2008) **Molecular mechanism for the umami taste synergism** *Proc Natl Acad Sci U S A* **105**:20930–20934 Google Scholar

Author information

Nanako Atsumi[†]
Graduate School of Medicine, Dentistry and Pharmaceutical Sciences, Okayama University, Okayama, Japan

[†]These authors contributed equally to this work.

Keiko Yasumatsu[†]
Oral Health Science Center, Tokyo Dental College, Tokyo
ORCID iD: 0000-0002-1911-8792

[†]These authors contributed equally to this work.

Yuriko Takashina
School of Pharmaceutical Sciences, Okayama University, Okayama, Japan

Chiaki Ito
Graduate School of Medicine, Dentistry and Pharmaceutical Sciences, Okayama University, Okayama, Japan

Norihisa Yasui
Graduate School of Medicine, Dentistry and Pharmaceutical Sciences, Okayama University, Okayama, Japan
ORCID iD: 0000-0001-7117-3070

Robert F. Margolskee
Monell Chemical Senses Center, Philadelphia, PA, USA
ORCID iD: 0000-0002-9572-2887

Atsuko Yamashita
Graduate School of Medicine, Dentistry and Pharmaceutical Sciences, Okayama University, Okayama, Japan
ORCID iD: 0000-0002-8001-4642

Corresponding author: Atsuko Yamashita, Graduate School of Medicine, Dentistry and Pharmaceutical Sciences, Okayama University, 1-1-1, Tsushima-naka, Kita-ku, Okayama 600-8530, Japan. Fax: +81-86251-7974. E-mail: a_yama@okayama-u.ac.jp.

Copyright

© 2022, Atsumi et al.

This article is distributed under the terms of the Creative Commons Attribution License, which permits unrestricted use and redistribution provided that the original author and source are credited.

Authors' response (18 October 2022)

> ***GENERAL ASSESSMENT***
>
> *The sweet and umami sensor proteins, taste receptors type 1 (T1Rs) are important GPCRs underlying taste sensation. In humans, amino acids bind and activate the T1r1/3 heterodimeric receptors leading to umami taste perception, whereas sugars activate the T1r2/3 receptors leading to sweet taste perception. In this manuscript, Atsumi and colleagues combine structural, biophysical and electrophysiological methods to show that Cl- ions also bind to T1Rs, at low mM concentrations, to evoke taste sensation. The authors (1) identify a putative evolutionarily conserved Cl- binding site in the crystal structures of isolated LBDs from medaka fish T1r2a/3 receptors, (2) show that Cl- ions promote protein stability and induce conformational changes in these mfT1r2a/3 LBDs, independent of orthosteric ligands, and (3) demonstrate that mouse chorda tympani nerves are activated by Cl- ions via a T1R-specific mechanism. Based on these findings, the authors conclude that low concentrations of Cl- may bind to sweet receptors and mediate the commonly reported sweet taste sensation following ingestion of low concentrations of table salt.*
>
> *The elucidation of the molecular mechanism(s) underlying salt taste sensation is a physiologically relevant question that will appeal to a broad audience. Moreover, the authors use an impressive array of different approaches to broadly cover numerous aspects, ranging from structural biology, to biophysics and physiological recordings. Overall, the identification of the chloride ion binding site is convincing, based on the previously solved structure, as well as the bromide ion substitution and long-wavelength Cl- anomalous difference analysis performed in this work. This analysis is supported by biophysical measurements showing that Cl- substantially stabilizes the wild type complex against thermal denaturation, but does not stabilize a point mutant in the putative Cl- binding site. The single fiber recordings suggest there is physiological relevance to the biophysical and structural findings, although they could be strengthened by additional control experiments. Overall, the possibility of Cl- ions acting as a sweet receptor ligand is enticing and the work will likely motivate additional research on this subject.*

The authors appreciate the positive assessment of the study, as well as the valuable comments and suggestions from the reviewers described below. Considering the referees' remarks, we performed additional control experiments and obtained evidence strengthening the T1r-mediated chloride sensing, as described below.

> ***RECOMMENDATIONS***
>
> ***Revisions essential for endorsement:***
>
> 1. *The authors should provide refinement statistics and methodology for both the Cl-- and Br-- bound structures, and some comparison between these two structures (global structural alignment & RMSD should be sufficient).*

We used the X-ray diffraction data from the Br–-substituted crystal, as well as the long-wavelength data from the Cl–-bound crystal, to draw the anomalous difference-Fourier maps pinpointing the Br–/Cl– positions. The structure models used for phase calculation were obtained by molecular replacement as described in the "Crystallography" section in the Materials and Methods. To show the certainty of the molecular replacement solutions, we added the *R*-factors for the models in the last sentence of the section. Since the resolutions for these anomalous data were limited and the structural comparison between the Br–-bound

and the Cl–-bound forms is not the main subject of the study, no further extensive structural refinement was performed on these data.

> 1. *We would recommend that the authors perform nerve recordings using artificial saliva rather than water as the perfusate. This is a key point because the chloride concentration in saliva is approximately 15 mM. Thus, according to their binding data, most T1rs should have chloride bound at baseline. Perhaps this means that chloride binding is required to allow sucrose or other ligands to cause sufficient conformational changes and receptor activation? If this is the mechanism, it would still be quite interesting, but would change the framing/interpretation as presented in the manuscript. If additional experiments are not feasible, the authors should carefully discuss this point.*

The authors thank the reviewers' insightful comments. We addressed this point and the results were shown in Figure 4D in the revised manuscript (Figure 3C in the original manuscript) and the third paragraph in the "Taste response to Cl– through T1rs in mouse" section in Results (p. 16, the next paragraph to the Figure 4 in the manuscript). As shown in Figure 4D, solely l-Gln or sucrose application in the absence of chloride (shown as l-Gln or sucrose) induced nerve responses. When those were applied in the presence of 10 mM chloride (shown as l-Gln+NMDG-Cl or sucrose+NMDG-Cl), the responses were increased to the similar levels as the summation of the response of the independent application of each substance. These results suggested that the chloride binding is not required for the receptor activation by sugars or amino acids, and that the binding of the two can occur simultaneously but does not cause synergistic responses.

> 1. *Some of the conclusions would be strengthened by additional control experiments, especially for the data obtained using FSEC-TS (Fig. 2C) and single fibre recordings (Fig. 3). For instance, how specific is the T105A mutation in abolishing Cl--dependent conformational changes? Did the authors check how the T105A mutation affects the ability of the LBD to undergo conformational changes in response to (1) L-Gln only and (2) Cl- only? Have the authors tried running these experiments at lower Cl- concentrations? 304 mM Cl- (page 16, line 363) is much higher compared to the effective concentration range claimed by the authors. For the single fibre recordings, have the authors tried applying 10 mM NMDG-gluconate? Having this negative control will provide more confidence in the specificity of Cl--induced impulses. Also, we would recommend a demonstration of reversibility in the gurmarin effect shown in Fig 3A.*

The authors thank the reviewers' important suggestions.

We performed a FRET assay for T1r2a/T1r3(T105A) mutant, and the results have been added to Figure 3E. In this experiment, we used 10 mM chloride, not ~300 mM, for both the T105A mutant and the wild-type LBD proteins and compared the results of the two. We confirmed that the extent of Cl–-dependent conformational change for the mutant was significantly reduced, as judged by the FRET index change. However, we also performed the same experiment using solely l-Gln as a titrant as the reviewers' suggested, and found that the amino acid-dependent change of the mutant was also significantly reduced. Therefore, although the former result itself agrees with our hypothesis, we are aware that the possibility of the entire protein deactivation during preparation cannot be excluded. Therefore, we presented the result with a notion about the study's limitations, as shown in the third paragraph in the section "Cl–-binding properties in T1r2a/T1r3LBD" in the Results (p. 12, the next paragraph to Table 1 in the manuscript).

Regarding the single fiber recordings, we performed the NMDG-gluconate application and confirmed that it did not induce significant responses at least up to 10 mM, as shown in Figure 4B. In addition, we described the method and results of our reversibility confirmation

test for gurmarin inhibition in the section "Single fiber recording from mouse chorda tympani (CT) nerve" in Methods (the last paragraph of the section, p.25).

> ***Additional suggestions for the authors to consider:***
>
> 1. *The introduction would benefit from greater focus and clarity to make the work more accessible to readers. Despite the overall focus on T1rs, only a quarter of the introduction revolves around these receptors. Additional information would help the reader to understand the research topic. For example, how many isoforms are there? Are these receptors obligate heterodimers? How similar are the mf T1r2a/3 compared to the human T1r2/3 receptors? If mf T1r2a/3 receptors are activated by amino acids, how useful a proxy are they in understanding sweet-sensing human T1r2/3 receptors? If T1r3 is found in both heterodimers, and amino acids bind to T1r3, how do these receptors discern between sweet and umami taste? What are the mechanisms underlying activation of these receptors? How are these receptors usually studied functionally?*

We agree with the significance of the information pointed out by the reviewers, and several points are currently under investigation in the field. However, we decided to keep the current contents in the Introduction due to the length limitation imposed by the submitted journal.

> 1. *Given the focus on isolated LBDs of (non-human) mfT1r2a/3 receptors, the authors are encouraged to comment on the probability of Cl- binding, and the subsequent conformational rearrangement observed in the isolated LBDs, actually translating to activation of (full-length) human receptors (and ultimately taste stimulation). Since the authors have previously assessed the function of hsT1r2/3 in HEK293 cells using Ca2+ imaging (PMID: 25029362), evaluation of the activation properties of Cl- at full-length receptors and testing the effects of T1r3 mutations on these Cl- effects would help to strengthen the manuscript. Also, there are several reported polymorphisms in the gnomAD database around the Cl- ion binding site (Thr102Met, Gly143Arg, Pro144Ser/Leu), so it would be interesting and helpful to test the effects of these variants that are found in the population. We do not expect the authors to perform these experiments, but in the absence of more conclusive functional data on full-length receptors, the authors should consider discussing these potential caveats in the text.*

The authors thank the reviewers' suggestions. We attempted the Ca2+-imaging in the early stage of the study, but it failed due to the instability of the cellular responses under the Cl–-depleted conditions. In contrast, nerve recordings are durable under a wide range of conditions. We described the situation in the first paragraph in the section "Taste response to Cl– through T1rs in mouse" in the Results. To verify that the nerve responses were attributed to T1rs, we confirmed that the chloride-dependent responses were attenuated by gurmarin, a T1r-specific blocker, and in T1r3-knockout mice, which were added in the revised manuscript.

Furthermore, we additionally performed a mouse behavioral assay and confirmed the preference for the solution containing chloride relative to H2O, which was again abolished by gurmarin. The results supported our discussion that the chloride is detected through a taste signal transduction pathway mediated by T1rs, as described in the last paragraph of the same section, and shown in Figure 4E, F.

The authors thank the reviewers' interesting and thoughtful pointing about the polymorphism, which is worth to be addressed in future studies.

> 1. *Given the availability of AlphaFold Multimer and the well-defined stoichiometry of the complex, did the authors attempt to predict a model of the full-length heterodimer? This may be informative with regards to the mechanism of signal transduction to the transmembrane domain.*

The authors appreciate the reviewers' helpful suggestion. We have constructed the full-length heterodimer models of T1rs from several species. We hope we will utilize the knowledge derived from them in our future studies.

> 1. *The nerve recording data would be more convincing if the authors could provide electrical recordings to truly sweet compounds at physiologically relevant concentrations (sucrose and artificial sweeteners). Currently, they only show data for 20 mM L-glutamine, which is not particularly sweet in Fig 3a-b, and then summary data for sucrose in Fig 3b.*

The authors thank this comment. We added representative recordings of the sucrose data in Figure 4A.

> 1. *The authors may wish to include a comment about whether bromide has the same effect on taste perception as chloride, and point out that gurmarin is a non-selective antagonist. Ideally, the nerve recordings should be done in T1r knockout mice to formally prove the mechanism. Although this may be beyond the scope of this work, a brief mention of this caveat seems warranted.*

As described above, we added the nerve recording data using T1r3-KO mice and proved that the chloride-derived responses were attributed to T1rs.

We agree with the reviewers' pointing that a halide-specificity to T1rs is an interesting issue to be addressed in future studies.

> 1. *Finally, the discussion would benefit from additional mention of ligand binding in relevant heterodimeric class C GPCRs, as well as the observation that chloride appears to work via a distinct mechanism despite its binding site being spatially very close to that of Gln.*

The discussion regarding the chloride-dependent regulation of ligand-binding in other class C GPCRs as well as structurally related receptors (ANPRs) was described in the last paragraph of the Discussion. The relationship between the amino acid-binding and the chloride-binding was addressed in the third paragraph in the "Taste response to Cl– through T1rs in mouse" section in Results (p. 16, the next paragraph to the Figure 4 in the manuscript).

(This is a response to peer review conducted by Biophysics Colab on version 1 of this preprint.)